JMEPEG (1994) 3:527-539

A Novel System to Study Wear, Friction, and Lubricants

M. Maamouri, J.F. Masson, and N.J. Marchand

A novel enclosed (pressurized) multispecimen wear testing system was designed and built to allow the fully computerized on-line measurement and control of friction, wear, and lubricants of different materials (metals, ceramics, composites, and plastics). This system is described in detail. The tribological parameters can be adjusted and controlled to reproduce the actual conditions that prevail in machine components. Several examples of the capabilities of the system are presented, with emphasis on measurements pertaining to wear, friction, and wear rates of self-lubricated ceramics as well as measurements of the efficiency of additives.

Keywords
friction, materials testing, testing, tribology

1. Introduction

CURRENT trends in design call for economical uses of materials. At the same time, end users have become more demanding and manufacturers now face stringent requirements in term of liability and product reliability. Testing engineers must, therefore, devise means of assessing the reliability of the manufactured product. The methods of so doing, for many applications involving contact between components, is to use wear tests (Ref 1).

In the wear testing of materials, the closer the test conditions approach those found in actual service, the more valid are the test results. Another chief limiting requirement for testing is that the test system must be fairly easy to use and run, and also free of uncontrolled variables.

Many testing laboratories (Ref 2) have used this approach in studying the suitability of materials for some given conditions, especially in the automotive and aviation industries and allied industries. However, current requirements in materials wear testing are such that relevant on-line measurements of wear and friction under various conditions, especially those that reproduce the actual conditions that prevail in engineering machineries, are urgently needed.

Hence, this paper presents a newly developed wear testing machine, capable of reproducing the tribological conditions prevailing in transportation and industrial machinery. The procedures for studying all kinds of materials (metals, ceramics, polymers, etc.), as well as for measuring the antiwear efficiency of lubricants and additives, are also presented in detail. The examples shown in this paper are presented not to emphasize the use of a given type of material or lubricants, but rather to illustrate the many capabilities of this newly developed system.

M. Maamouri, J.F. Masson, and **N.J. Marchand,** Laboratoire de Tribologie - Département de Métallurgie et de Génie des Materiaux, École Polytechnique, Montréal, Canada, H3C 3A7

2. Description of the Experimental Apparatus

Details of the experimental system are illustrated in Fig. 1. The apparatus consists of a horizontal multispecimen tester, a hydraulic cylinder, an electric motor and power control system, a gear box, a hydraulic lubrication loop circuit, and a computerized data acquisition and control system.

The multispecimen tester is enclosed in a pressurized chamber for controlling the tribological variables. It involves a horizontal rotating table on which a flat interchangeable disk is settled to guarantee the most accurate results in wear testing for a variety of materials (including metals, plastics, ceramics, and most composites). Three samples are used, which can either be hemispherical pins, spherical balls, roller-type pins, cylindrical pins, etc. They are fixed in a specimen holder, sliding in a circular path (wear track) on the surface of the disk. The holder can also accommodate rings of different cross-sectional shapes.

The normal load is applied by a hydraulic cylinder and is sensed by a load cell that is mounted between the specimen holder and the hydraulic cylinder. The load cell and its proportional-control valve (which is mounted on the hydraulic unit) allow the load to be fixed to the required wear force from 0.4 to 455 kgf (1 to 1000 lb).

The electric motor (7.5 hp and 1800 rpm) coupled with a 5:1 reducer gear box is able to provide sliding velocities ranging from 0.4 to 5 m/s (30 to 360 rpm on a 0.27 m diameter wear track). Furthermore, any intermediate velocities can be selected and regulated by the digital power controller via the computer system.

The hydraulic lubrication loop circuit, which can use any type of lubricants, consists of a 300 mm × 300 mm × 300 mm oil reservoir, a pressure pump operating at pressures up to 27.56 bar (400 psi) and 4.5 L/min (1 gL/min), a flow meter, and a heat exchanger. To allow any given pressure at a given flow rate, a pressure valve is also mounted on the lubrication loop circuit, between the test chamber and the oil reservoir.

Two pressure sensors are used. One is installed in the vicinity of the wear pins (PI, pressure sensor I in Fig. 1) to record the pressure of the hydrodynamic lubricant film beneath the samples, and the second is installed in the chamber (PII, pressure sensor II in Fig. 1) to measure the bulk pressure. Because the pressure of the lubricant in the test chamber is generally higher

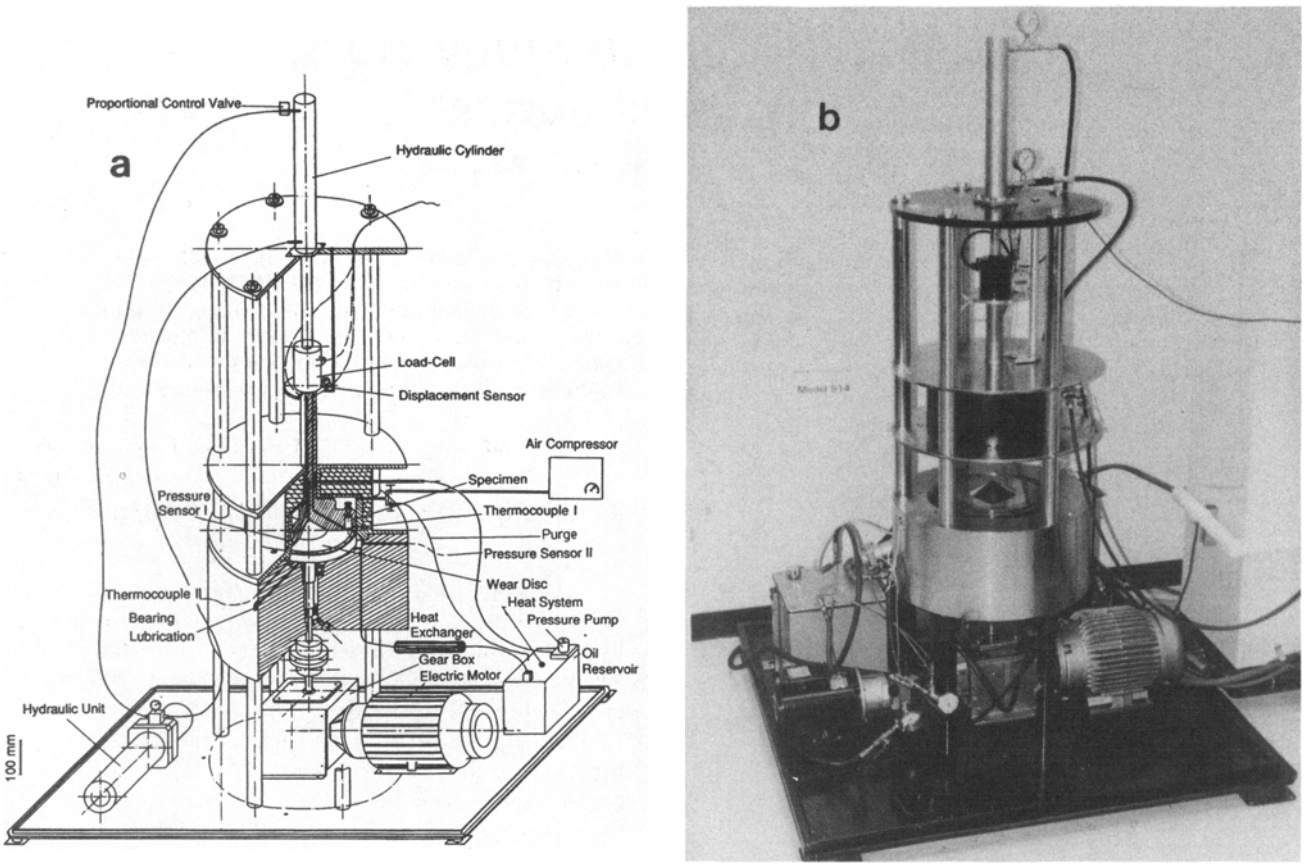

Fig. 1 Schematic diagram (a) and photograph (b) of the enclosed multispecimen wear testing machine

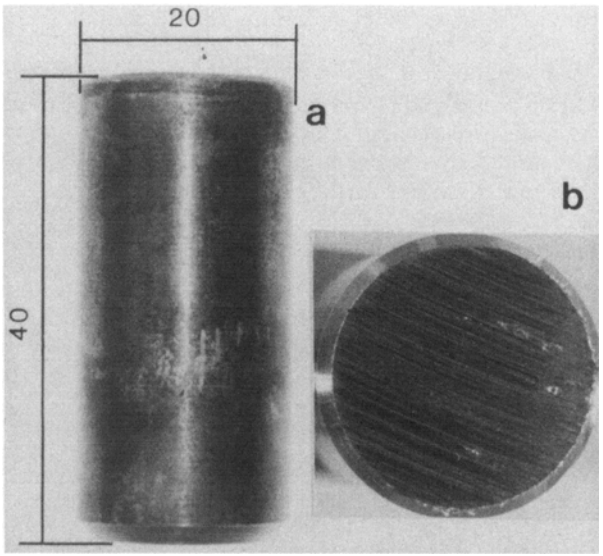

Fig. 2 (a) Selected specimen configuration and (b) aspect of the worn surface (note the uniformity of wear)

than the atmospheric pressure, the sensed load (load cell) is not the actual load experienced by the specimens, due to the vertical hydraulic reaction of the pressurized lubricant. An electronic compensation is carried out to determine accurately the precise wear load, as described in a following section.

Three thermocouples (I, II, and III) are mounted to measure respectively the temperature of the wear pin surface (T_s), the temperature of the oil in the chamber (T_c), and the temperature of the oil in the reservoir (T_r) (which can be heated and controlled between 20 °C and 250 °C).

The hydraulic lubrication loop circuit was designed to allow the installation of other tribological and wear-detecting devices, such as viscometers and ferrographs, to provide more information regarding the state of the lubricant and/or the state of wear of the materials being studied.

The entire system (1350 kg or 3000 lb) is mounted on a platform that lies on antivibration fixtures, to ensure that vibrations do not affect the tests. It is the antivibration capability of the system that allows wear to be measured on-line by a displacement sensor device with a resolution better than 1 μm. This sensor is mounted at the top of the specimen holder. The accuracy of the measurements is proof-checked regularly using a microbalance (resolution of 0.1 mg) at the end of the wear tests (this gives the total amount of wear in the form of a single number).

2.1 *Selection of Specimen Configuration*

The selected specimens are cylindrical and flat-ended pins with an area of contact of about 300 mm^2 (Fig. 2a). Because three samples are tested simultaneously, the total surface of material studied is significant (9.0 cm^2), ensuring that the measurements represent realistic averages of the material responses under friction wear conditions. This is particularly important

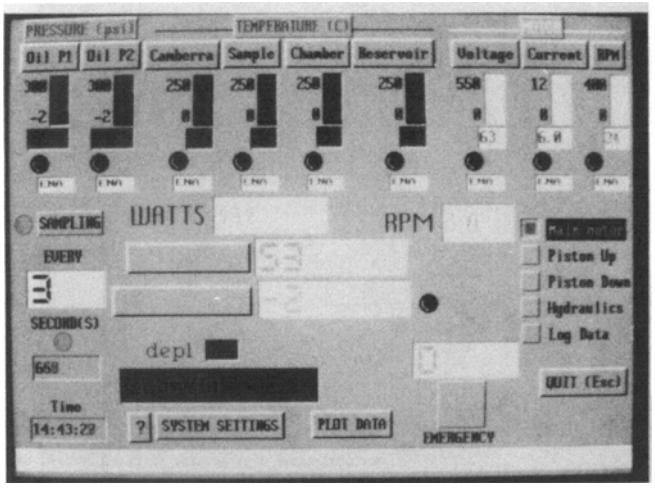

Fig. 3 On-line computer display of the tribological parameters

when trying to assess the wear characteristics of a given microstructure. This flat-ended pin geometry was selected over spherical balls or hemispherical pins because these geometries produce accelerated results due to the fact that the load is applied over a small contact area. The volume of material that is lost is not (and cannot be) proportional to the recorded displacement.

The wear disk is large enough (the wear track is 27 cm in diameter) to guarantee a uniform parallel wear motion over the complete surface of the pins (Fig. 2b). The use of such a large wear track also entails significant torque, which is easily sensed by the electric motor power controller. Most conventional wear testing machines use needle-type specimens (or hemispherical pins) and small rotating disks (Ref 3, 4), so a very small amount of material is studied. Furthermore, as wear occurs, the surface being tested changes, as well as the local velocities, because of radius changes. This renders many pub-

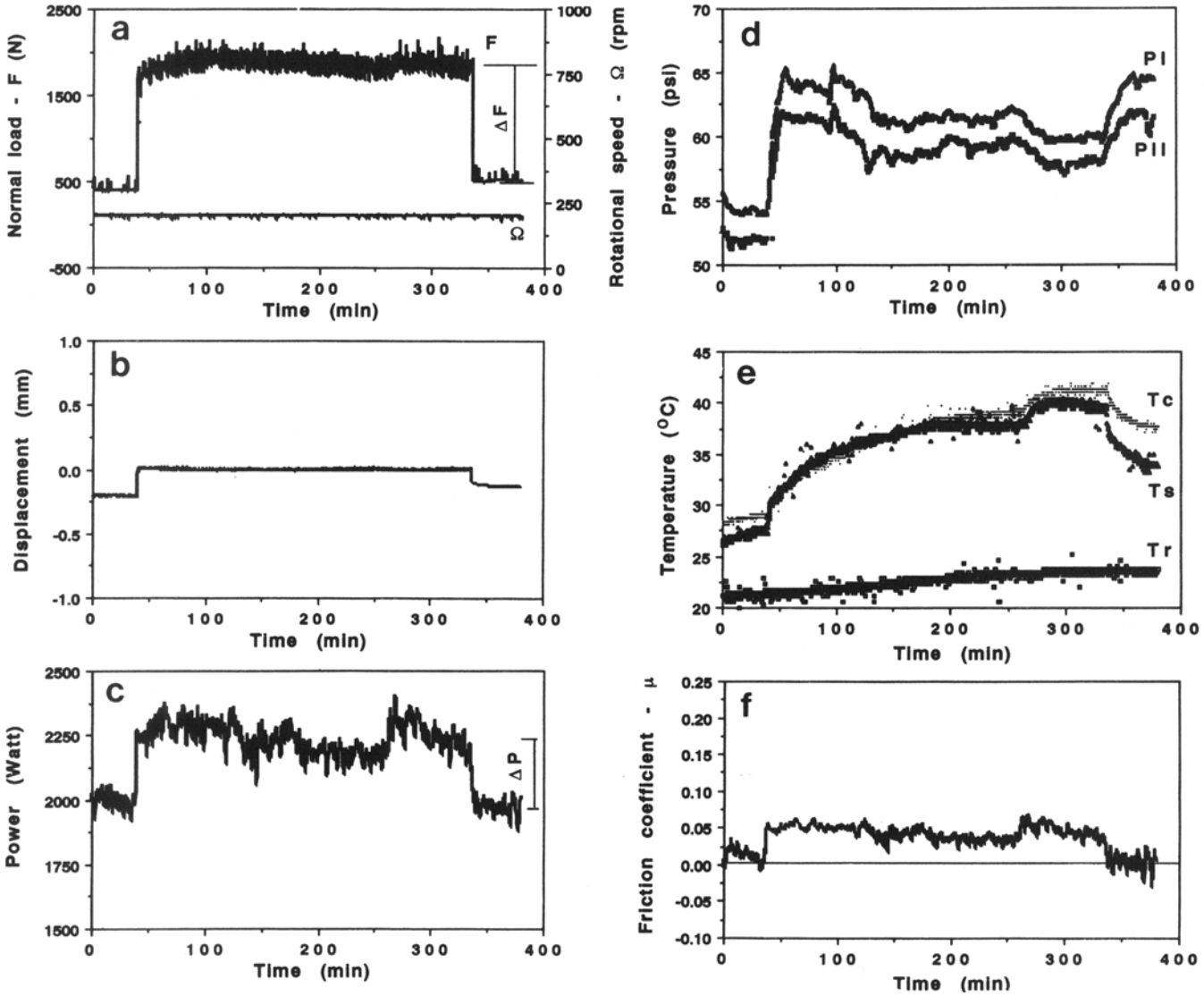

Fig. 4 Measured wear parameters vs. real time (M50/AISI 52100 bearing steels). (a) Normal load F (ΔF is the real normal load) and rotational speed (Ω). (b) Displacement d. (c) Electric motor power (ΔP results from ΔF). (d) Pressures of the lubricant film beneath the wear pins (PI, pressure sensor I) and in the test chamber (PII, pressure sensor II). (e) Temperature of the sliding contact (T_s), in the test chamber (T_c), and in the oil reservoir (T_r). (f) Friction coefficient μ

Table 1 Nominal compositions of M50 and AISI 52100 bearing steels

Materials	Composition, %					
	C	Mn	Si	Cr	Mo	V
M50	0.85	...	...	4.10	4.25	1.00
AISI 52100	1.04	0.35	0.25	1.45	...	...

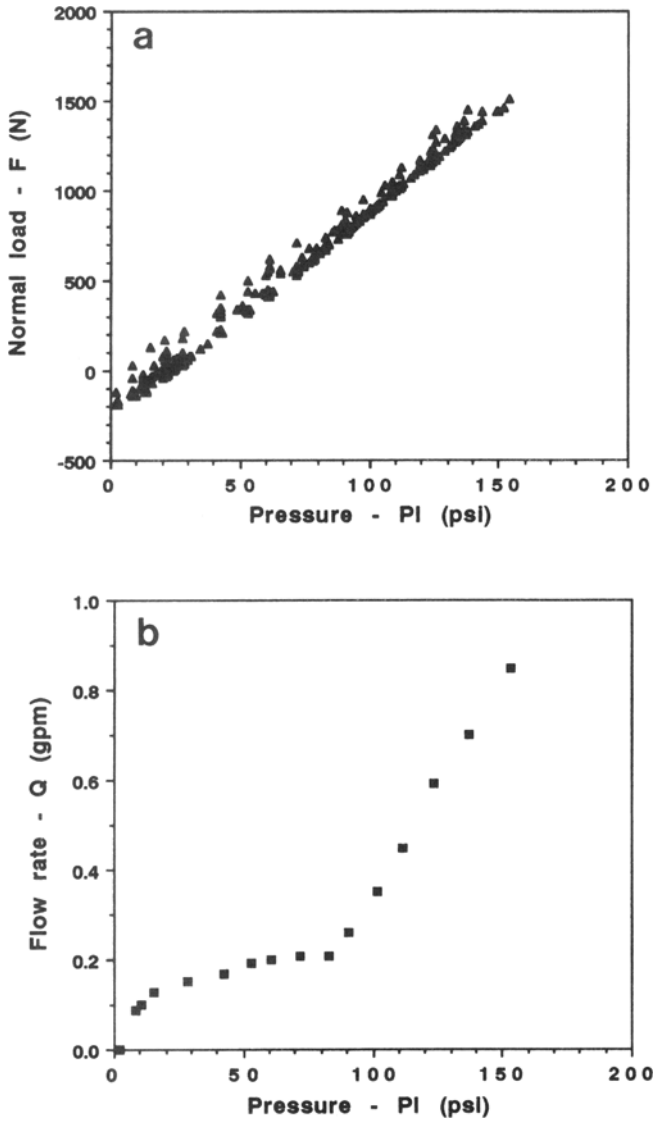

Fig. 5 (a) Hydraulic compensation load (F) vs. lubricant film pressure (PI). (b) Flow rate (Q) vs. lubricant film pressure (PI)

lished data questionable, especially those pertaining to the measurement of friction (μ) and the measurement of wear rates.

2.2 *Computer Data Acquisition System*

The tribological data from the wear system are monitored (Fig. 3), manipulated, and stored by a computerized data acquisition system. The system consists of a 486 computer and a specially built electronic analogue/digital controller. The computer, driven by a dedicated software, displays, manipulates, and stores the data in a meaningful format. Via the controller, it samples many channels at selected time intervals. The data pertaining to a specific parameter can also be visualized on-line in detail (adjustable scales) without affecting the test or losing any other data (other channels). The data can also be transferred to any spreadsheet program for further analysis and graphing. Thus, with the present data acquisition system, the data are recorded, manipulated using on-line statistical analysis, stored, and plotted (or graphed).

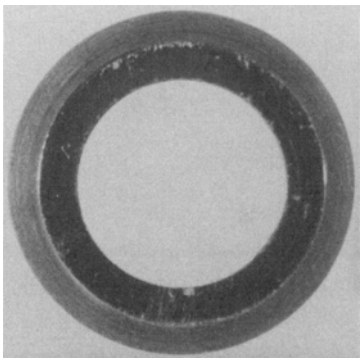

Fig. 6 Specimen configuration for the ceramic/metal plasma spray coating studies. Note the ceramic sample (white circle) embedded in the metal pin.

3. Capabilities of the System

In this section, we present some examples of utilization of the wear testing bench. Measurements are presented for wear, wear rate, and friction of various tribological systems (M50/AISI 52100, ceramic/metal plasma spray coating) as well as the efficiency of a given additive for minimizing wear and friction. These examples illustrate some of the capabilities of this advanced wear testing bench.

3.1 *Measurements of wear, wear rate, and friction (M50 on AISI 52100 bearing steels)*

Figure 4 illustrates the different wear parameters being recorded during the testing of M50 (AMS 6491A), a high-temperature bearing steel, sliding against AISI 52100, a high-carbon bearing steel. Table 1 lists the compositions of these selected steels (Ref 5).

Here the system was set at 200 rpm (2.8 m/s) and 1.8 L/min (0.4 gL/min). The following procedure is used to determine the friction coefficient (μ) and wear rate of this tribosystem.

After adjusting the rotational speed and the oil pressure to the desired value (while holding the pin specimen out of contact with the disk), the specimen holder is brought close to the surface of the disk (about 200 μm away, Fig. 4b) without touching it, as per ASTM standard G-99. In order to achieve this, the

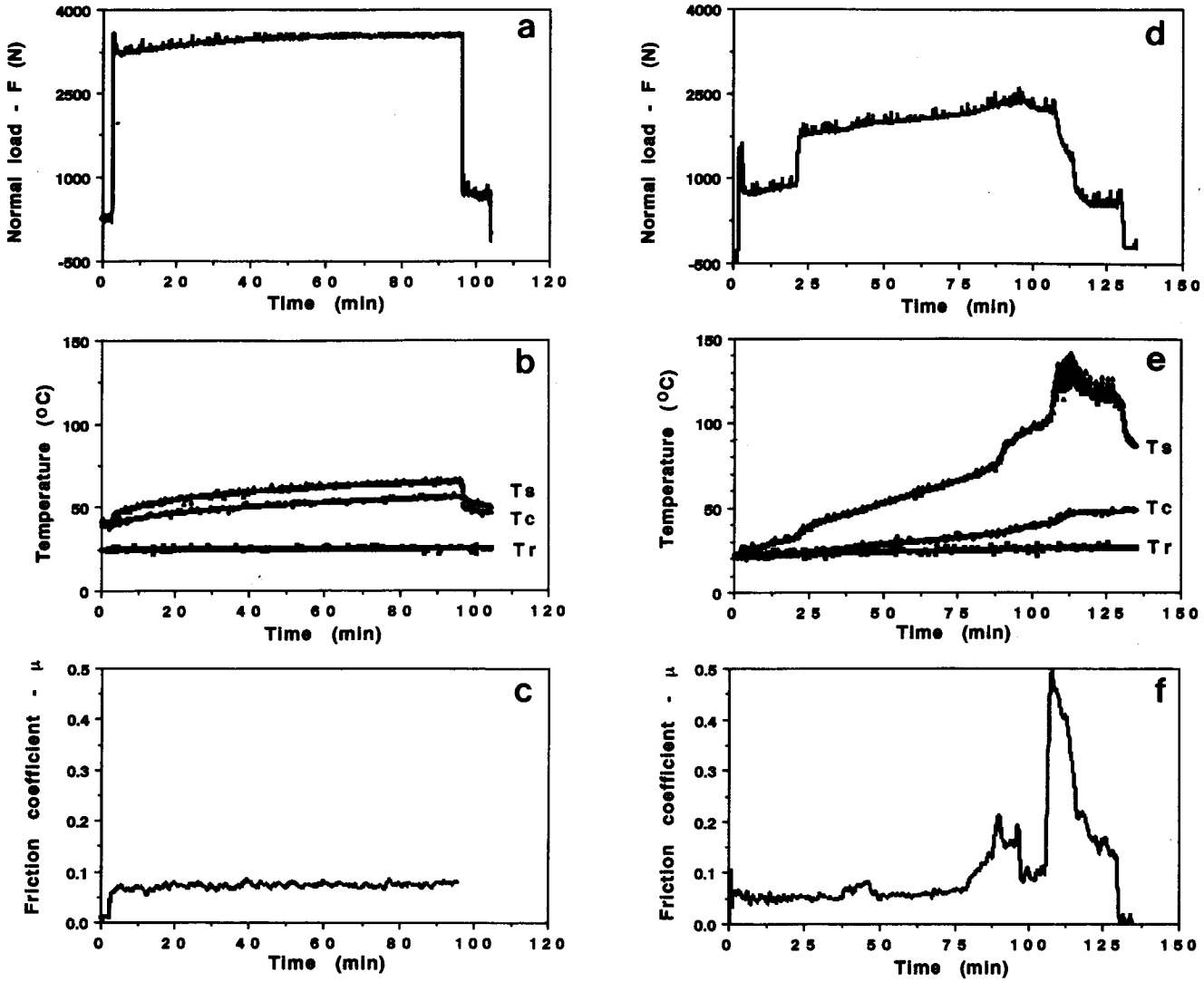

Fig. 7 Results of the wear tests for pure alumina in lubricated sliding (a, b, and c), and for alumina with 8.8 wt% graphite in unlubricated sliding (d, e, and f)

normal load applied by the piston needs to be increased. However, the recorded load to obtain these conditions (Fig. 4a, 4d) corresponds to overcome the hydraulic pressure of the lubricant (hydraulic compensation). An overload ΔF (Fig. 4a) corresponds to the real normal force applied on the samples.

Figure 4(c) shows the power of the electric motor as a function of time. The overload ΔF increases the power ΔP. Therefore, the friction coefficient (Fig. 4f) can be calculated from the real normal load ΔF and the corresponding electric motor power variation ΔP. These computations are carried out on-line and can be displayed. In this new wear system, the changes in the coefficient of friction can be easily measured as a function of any tribological parameter. For example, the increase of the coefficient of friction shown in Fig. 4(f) is associated with the pressure drop of the lubricant in the test chamber. The thermocouples in the test chamber and beneath the surface of the samples show a corresponding increase in the temperature (Fig. 4e).

Figure 5(a) shows the hydraulic compensation load as a function of the lubricant pressure in the vicinity of the samples. The curve is linear and the negative values correspond to the weight of the specimen holder.

Figure 5(b) illustrates the change of the flow rate Q as a function of the pressure when the pressure valve is fully open. Two distinct areas are clearly visible. In the low-pressure region ($P < 90$ psi), a significant change in pressure can occur by a small change in the flow rate. By contrast, when the pressure is high ($P > 90$ psi), every change in pressure induces a significant change in the flow rate. Finally, as shown in the particular example, the wear rate can be controlled by the normal load and/or the oil pressure.

3.2 *Measurement of wear, wear rate, and friction (ceramic/metal plasma spray coating)*

3.21 Sample Preparation

One set of specimens was fabricated from pure alumina powder. The other set was fabricated from a mixture of alumina and 8.8 wt% graphite. These powders were hot pressed for 1 h

at 1600 °C under a pressure of 10 MPa in graphite dies to form 60 mm diameter cylinders from which 10 mm diameter and 5 mm thick samples were prepared. Each disk sample was then mounted on a stainless steel pin housing of 20 mm diameter and 40 mm length (Fig. 6). The rotating disk was metal plasma spray coated to produce a hard wear resistant coating (Ref 6). The wear tests were carried out at 200 rpm (sliding velocity of 2.83 m/s) under unlubricated and lubricated conditions (60 psi Sunvis 732 from Sun Co., blend 1421). The normal load was set to 3000 N for both types of ceramics (pure alumina and alumina with 8.8 wt% graphite).

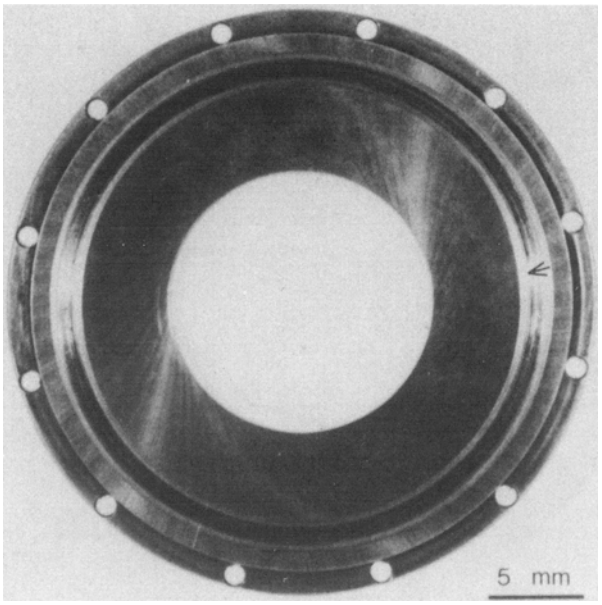

Fig. 8 Interchangeable wear disk. Note the aspect of the wear groove (arrowed).

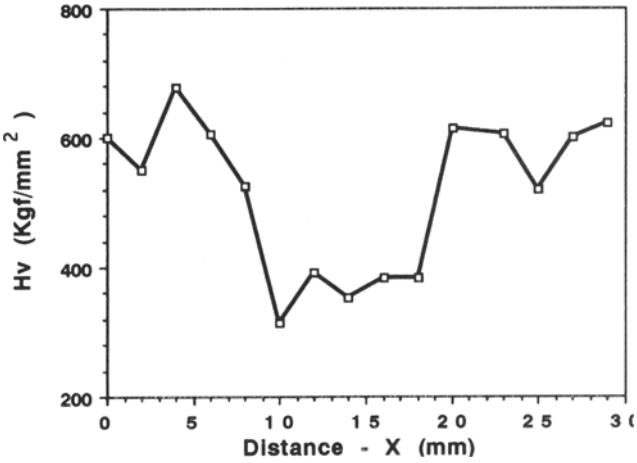

Fig. 9 Microhardness profile across the wear groove

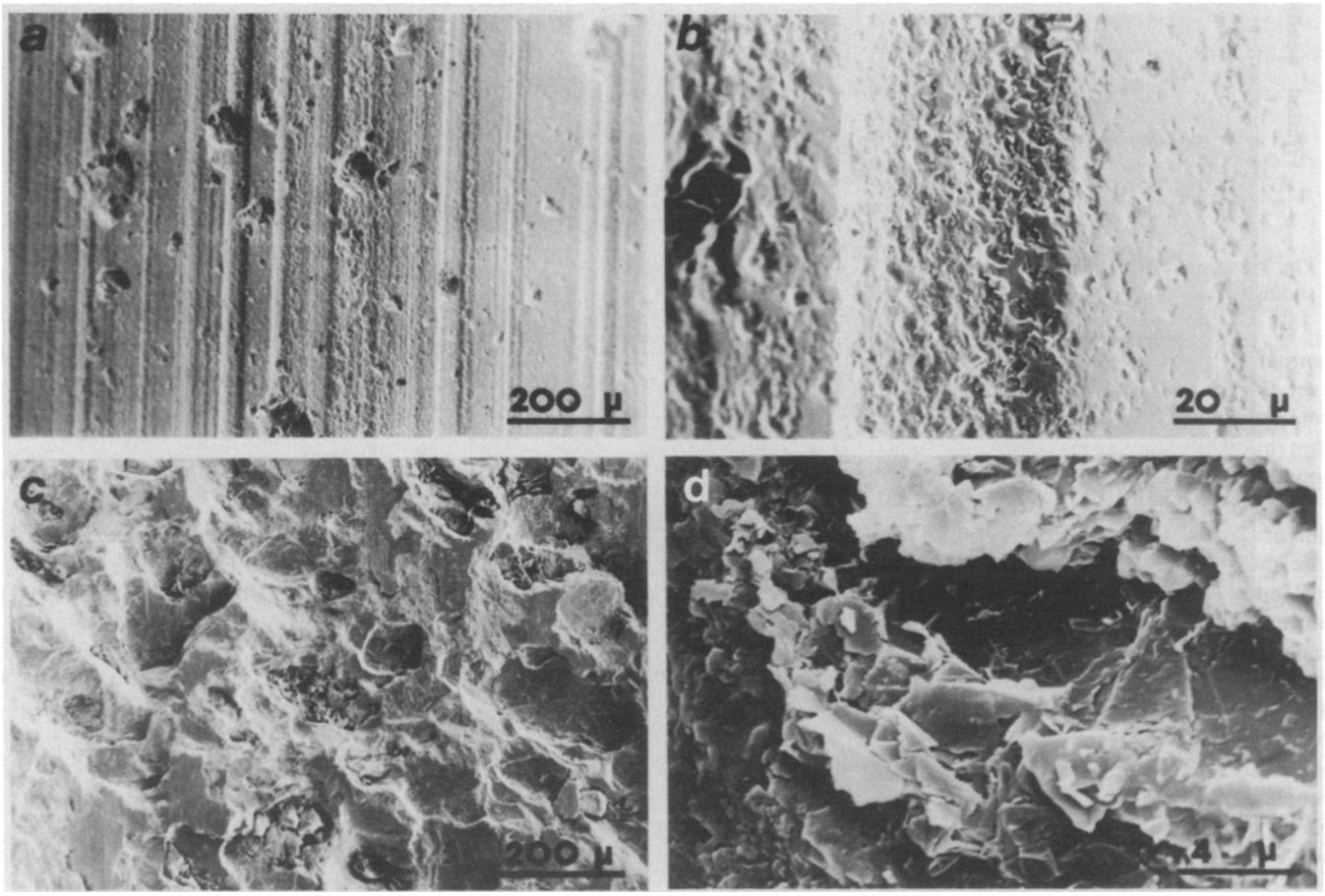

Fig. 10 Aspect of worn pure alumina in lubricated sliding (a and b), and of worn alumina with 8.8 wt% graphite in dry sliding (c and d)

The aim of these experiments was to verify whether ceramics containing graphite (e.g., 8.8 wt% graphite) with self-lubricating properties behaved in service as well as lubricated metal/metal systems or lubricated alumina/metal coating systems. Obviously, tribological systems operating without lubricants would generate significant savings.

3.22 Results—Friction

Figures 7(a) to 7(c) show the data pertaining to pure alumina (sliding against the metal plasma spray coating) in the lubricated conditions. Figures 7(d) to 7(f) show the results for the alumina with 8.8 wt% graphite tested under dry sliding contact (unlubricated) against the metal plasma spray coating. As can be seen, the alumina and the alumina with 8.8 wt% graphite have the same coefficient of friction ($\mu = 0.06$) (Fig. 7c and 7f), although pure alumina was tested under lubricated conditions and alumina with 8.8 wt% graphite was tested without any lubricant (dry). However, the friction coefficient of alumina with 8.8 wt% graphite was found to sharply increase at the end, where scuffing failure occurred (Fig. 7f). Accordingly, thermo-

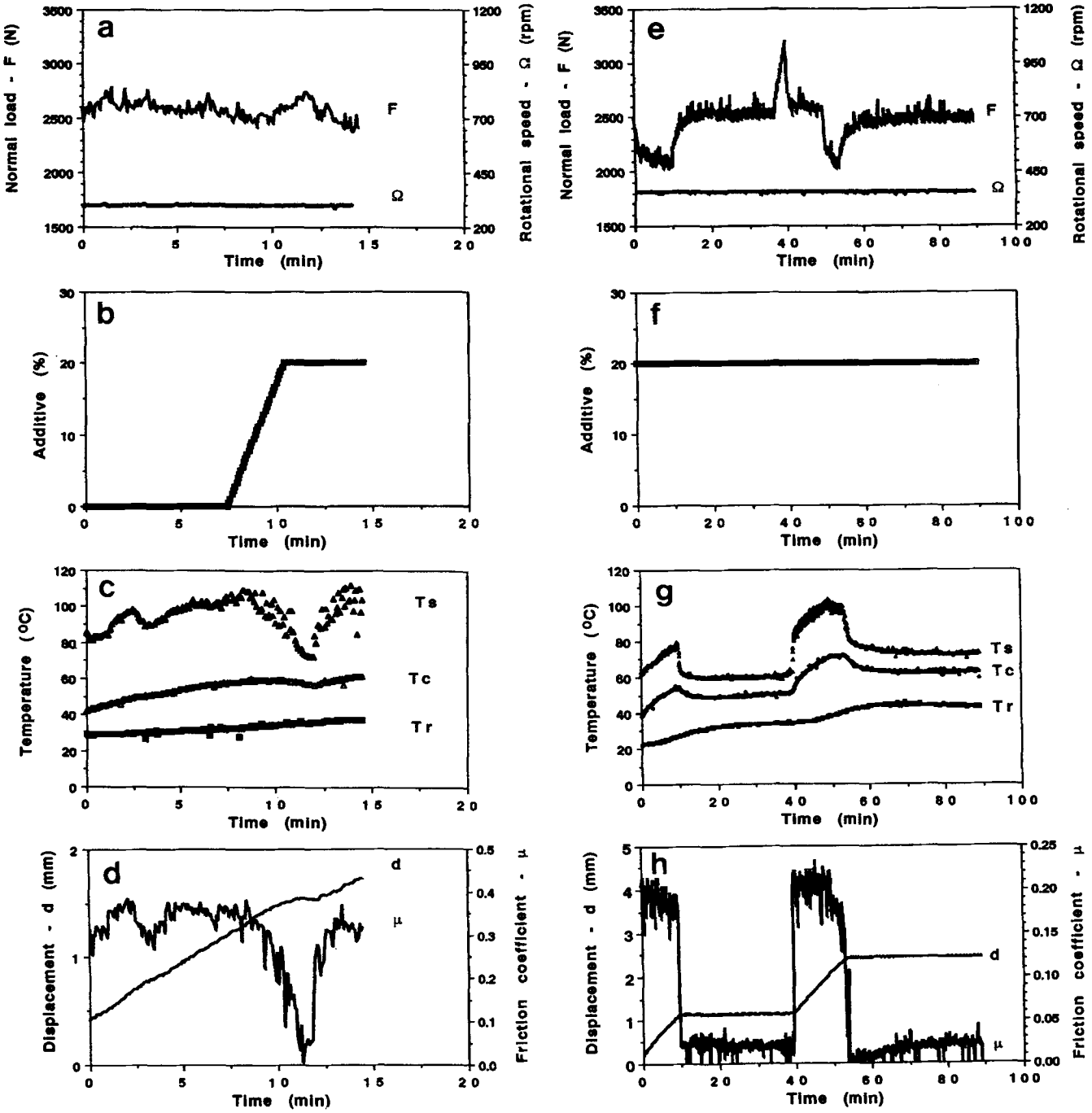

Fig. 11 Additive efficiency measurements. Determination of the optimal amount of additive (a, b, c, and d); Determination of the optimal working temperature (e, f, g, and h)

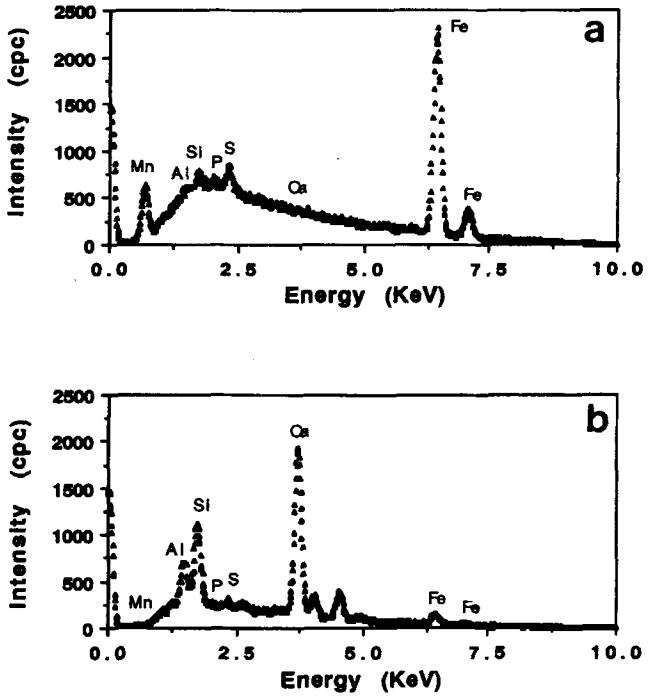

Fig. 12 Electron probe microanalysis of a worn surface in the case of severe wear conditions. (a) X-ray spectrum associated with smooth areas. (b) X-ray spectrum associated with the valleys

couple I recorded a rise in T_s, the temperature of the sliding contact zone (Fig. 7e). Measurements of the microhardness profile across the wear groove (see the arrow, Fig. 8) showed a significant drop of the hardness in the groove area (Fig. 9). This indicates that the plasma spray coating completely wore out, such that at the end the alumina graphite samples were sliding on the steel substrate.

3.23 Results—Wear Mechanisms

Representative scanning electron micrographs of the worn pure alumina and worn alumina with 8.8 wt% graphite are shown in Fig. 10. In particular, Fig. 10(a) and 10(b) show the wear aspect of pure alumina obtained under lubricated conditions (60 psi), while Fig. 10(c) and 10(d) correspond to alumina with 8.8 wt% graphite under dry sliding conditions. Microscopic examination of the worn surfaces indicated that the dominant wear mechanism of pure alumina (lubricated) is micropolishing. Numerous plowing grooves, all over the exposed surface, are seen in Fig. 10(a). In addition to plowing, localized fracture facets were found that contributed to wear (similar worn surfaces were observed after testing alumina with 8.8 wt% graphite in the lubricated condition). This contrasts with the wear mechanism found in alumina with 8.8 wt% graphite tested in the dry condition. In that case, extensive pull-out (extraction) of the graphite flakes resulted in the microfracture of the remaining alumina matrix, as shown in Fig. 10(c) and 10(d).

If microfracture of the alumina matrix can be retarded or avoided by using different sizes or geometries of flakes, the reliable use of unlubricated ceramic/metal plasma spray coating systems can be envisaged in a near future. All the results indicate that if the coating can be made more wear resistant, ceramics with graphite can be used in machineries and systems without lubricant, producing significant savings in weight and maintenance.

3.3 *Measurement of the Efficiency of an Additive*

Additives are expected to improve the lubricant ability of the base oils by either enhancing the desirable properties already present or adding new properties (Ref 7). For this reason, additives are an integral part of modern formulated lubricants. The general effectiveness or the operating range of these additives can be determined by quantitative wear testing.

It is well known that an increase in load or a decrease in rotational or linear speed promotes metal-to-metal contact. This causes a rise in temperature in the contact zone due to frictional heat. As a consequence, the lubricant loses viscosity, which decreases the film-forming ability of the lubricant and the ability to minimize metal-to-metal contact. Under these conditions, the nature of the lubrication changes from hydrodynamic to mixed-film to boundary (thin-film) lubrication. Antiwear additives and extreme pressure agents (EP) can offer protection under mixed-film and boundary condition.

Antiwear and EP additives provide protection by a similar mechanism, but the EP additives typically require higher activation temperatures and loading conditions. Simply stated, antiwear additives perform under mild conditions, while EP additives operate under severe conditions. The severity of an operating condition is determined by the "load factor" experienced by the additive and the temperature at which the additive is to function (heavy loading requires EP agents and mild loading requires antiwear agents). Thus, both the load and the temperature that are expected to be experienced in-service by the equipment or the machinery need to be considered before the antiwear and EP agents are selected (Ref 7).

Two wear tests were carried out, using the pressurized testing machine, to quantify the severity of conditions sustainable by an additive as determined by the load factor experienced by the additive. The temperature range of application of the additive was also determined. The M50 high-temperature bearing steel and the AISI 52100 high-carbon bearing steel were used to complete the tribosystem, because their structures allow high temperatures to be attained at the contact interface when the proper load and rotational speed are applied.

3.31 Effect of the Amount of Additive on the Tribological Parameters

Figures 11(a) to 11(d) show the tribological parameters as a function of real time for M50/AISI 52100 bearing steels in sliding lubricated conditions. The base lubricant used was Sunvis 732, blend 1421, and the additive was a basic calcium sulfonate. The AISI 52100 steel disk was rotated at 300 rpm (4.24 m/s), and the normal load was set to 2700 N (Fig. 11a). These conditions were imposed as to achieve a temperature T_s (in the sliding contact zone) of about 110 °C (Fig. 11c), for which the additive is expected to perform well. Then the additive was added in the reservoir (Fig. 11b) to determine the percentage of additive that significantly affects the tribological parameters at this fixed temperature.

As the amount of additive was increased, a decrease in T_s was recorded at an additive volume of 10%. The temperature

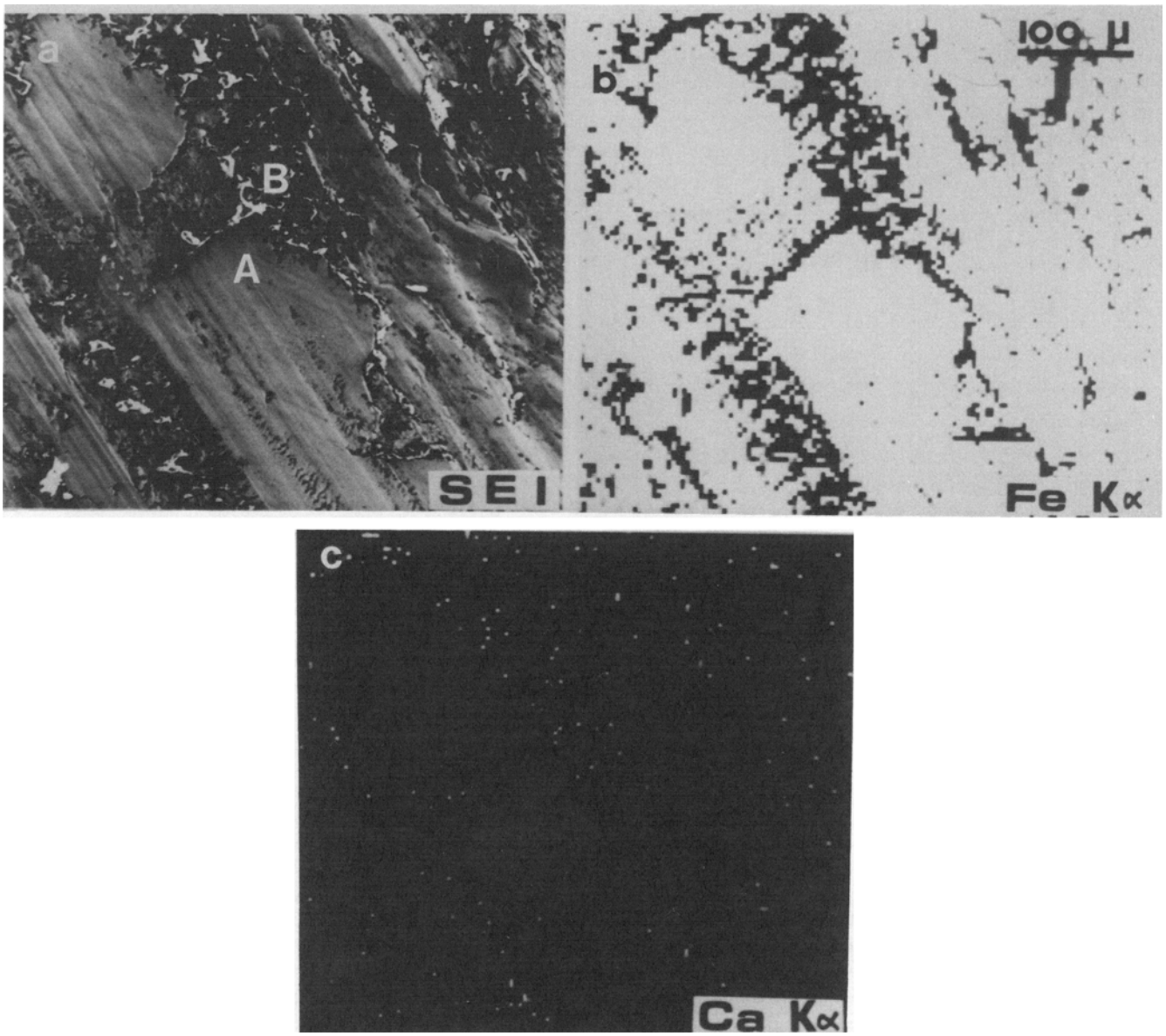

Fig. 13 Scanning electron micrographs. (a) Secondary electron image. (b) X-ray map of iron. (c) X-ray map of calcium

continued to decrease significantly up to 20% volume of additive (Fig. 11c). This decrease in temperature was found to result from a sharp drop of the coefficient of friction, which induced a very low wear rate (see curves "μ" and "d", Fig. 11d). For the selected testing conditions, the efficiency of the additive lasted for only a short time, after which the tribological parameters rose again to their initial states. This phenomenon can be explained by the thermal decomposition of the additive and by the forming of products that react with the metal surface to form a solid protective layer. This solid metal film covers the surface and fills the asperities, thereby reducing friction and protecting against welding and surface wear. However, if the wear testing conditions are severe enough to cause the breakdown of the protecting layer, metal-to-metal contact will occur, rapidly increasing the wear rate as measured in the initial case without additive.

To confirm the hypothesis that the efficiency of an additive is linked to the formation of a solid protecting film, electron probe microanalysis (EPMA) of a worn surface was carried out. Figures 12(a) and 12(b) show the x-ray spectrums associated with the smooth areas (zone A in Fig. 13a) and the rough zones (zone B in Fig. 13a), respectively. In the rough areas, which correspond to valleys, there is little or no iron but significant amounts of calcium. This indicates that the solid film was indeed completely removed except for a few fragments left in the asperities (scratches and valleys, etc.) that exist in the base metal. X-ray maps of iron (Fig. 13b) and calcium (Fig. 13c) further confirm the prior existence and failure of the solid film.

3.32 Effect of Temperature on the Efficiency of the Additive

Figures 11(e) to 11(h) show plots of the tribological parameters measured during lubricated wear testing of AISI 52100 (56

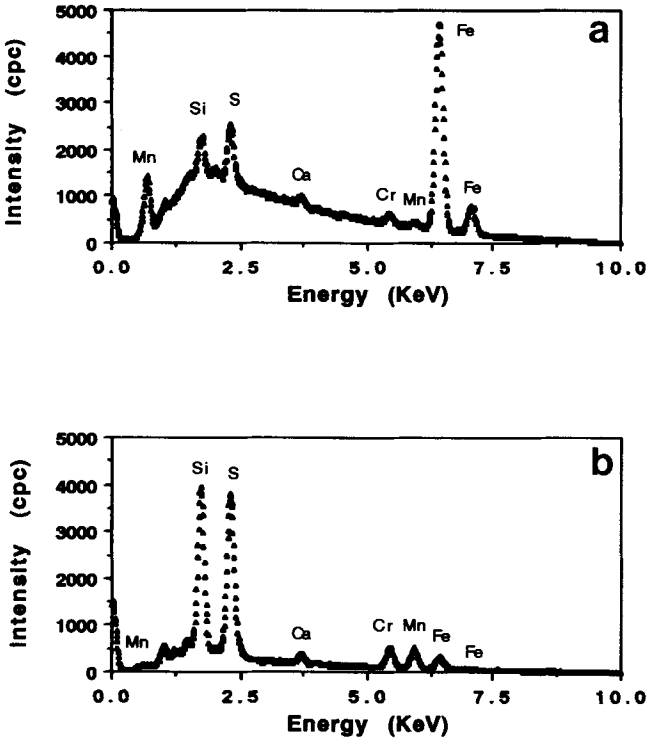

Fig. 14 Electron probe microanalysis of a surface for the case of "suitable" wear conditions. Spectra of the matrix (a) and the solid protecting layer (b)

HRC) against AISI 52100 (62 HRC). The AISI 52100 steel disk was rotated at 360 rpm (5 m/s) (Fig. 11e), and the lubricant used for the testing was a mixture of Sunvis 732, blend 1421 and 20% volume of a basic calcium sulfonate additive (Fig. 11f). The normal load was adjusted so that the contact temperature T_s increased slowly, as shown in Fig. 11(g). After reaching 80 °C, the temperature dropped sharply and quickly stabilized around 60 °C (up to 40 min). During this same period of time, the coefficient of friction decreased sharply (Fig. 11h) to a very low level, and the displacement sensor recorded a quasiplateau (Fig. 11h) indicating a very low wear rate.

To confirm that the formation of a solid film was also responsible for the low μ and low wear rate, the normal applied load was rapidly increased at 40 min while the rotational speed was kept constant (Fig. 11e). The temperature T_s, the friction coefficient μ, and the wear rate d increased sharply, indicating the breakdown of the protecting solid film. However, all these parameters dropped again to their low values when the normal load was reduced, thus allowing the formation of a new solid protective layer. The test was then stopped (at low values of μ and T_s) so that EPMA could be carried out on the worn surfaces. Figures 14(a) and 14(b) show the X-ray spectra corresponding to the matrix (zone A in Fig. 15a) and the solid protecting layer (zone B in Fig. 15a), respectively. As can be seen, sulfur is a major constituent of this protective layer while Ca seems to be low. However, x-ray maps of iron (Fig. 15b), sulfur (Fig. 15c), phosphorus (Fig. 15d), chlorine (Fig. 15e), and calcium (Fig. 15f) indicate that the solid layer, which was formed under the present testing conditions, is uniform over large flat areas, not in the valleys, as shown by Fig. 13.

The present results seem to indicate that the chemistry of the protective layer depends on the tribological conditions prevailing at the contact interface. Although very complex, the formation and breakdown of these protecting layers or films can be easily studied with this new wear testing system.

3.4 *Calibration of an On-line Debris Detection System*

Many interesting wear data have been obtained using thin-layer-activation techniques (TLA) (Ref 8, 9). The TLA method for wear monitoring consists of measuring changes of low-level radiation to quantify wear. As such, it involves the activation of one of the materials in contact, using a high-energy ion beam to produce radioactive isotopes. This method enables the quantity of wear debris to be measured, in real time, with the help of standard radioactive counting systems, such as NaI detectors equipped with readout instruments. To increase the sensitivity, simultaneous measurements of the increased activity in the lubricant (wear debris) and of the worn surface itself (residual) can be performed.

Several specimens of A304 stainless steel pins have been subjected to a 10 MeV proton activation beam under vacuum in a Tandem accelerator (Ref 10). A 0.07 mm^2 spot was exposed to the beam at normal incidence to the metal surface. For this energy level, ^{56}Co isotopes were produced from the transmutation of iron atoms. The activation layer had a depth of about 180 μm.

In the first experiment, one radioactive sample was used with the remaining two not activated. The samples were worn out slowly on a P20 tool steel disk. Radioactive decay measurements were taken using an NaI detector located in close proximity to a 3 μm oil filter. The average radioactivity lost from the pin surface, as well as the depth worn from the samples (as measured by the displacement sensor) are plotted versus real time in Fig. 16. It is clear that the two curves have the same trend, with the activation curve showing a plateau at about 180 μm, corresponding to the expected activation depth. Measurements of weight loss, at the end of the test, indicated that 90% of the wear debris were captured in the 3 μm filter. Figure 17 shows wear debris particles collected in the filter (Fig. 17a) and particles collected after the oil was filtered (Fig. 17b). As expected, the particles in the oil are much smaller than the ones captured in the filter.

In another experiment, the radioactivity in the lubricant (wear debris) and the residual radioactivity of the worn surface were measured simultaneously. Thus, two NaI detectors were used, one located in close proximity to the 3 μm oil filter and one located close to the irradiated pin. The curves in Fig. 18 indicate that the pressurized multispecimen machine is almost free of wear debris capture, because the radioactivity lost from the sample (curve b) corresponds to the radioactivity gained by the oil filter (curve a).

Our results indicate that if one knows the efficiency of capture of this type of filter and the actual measurements of wear (by the displacement sensor), the TLA method can be calibrated to allow fairly accurate measurements of wear. Of course, to be used in service, the TLA method requires that the same type of isotopes, oil filter, and γ-ray detection systems

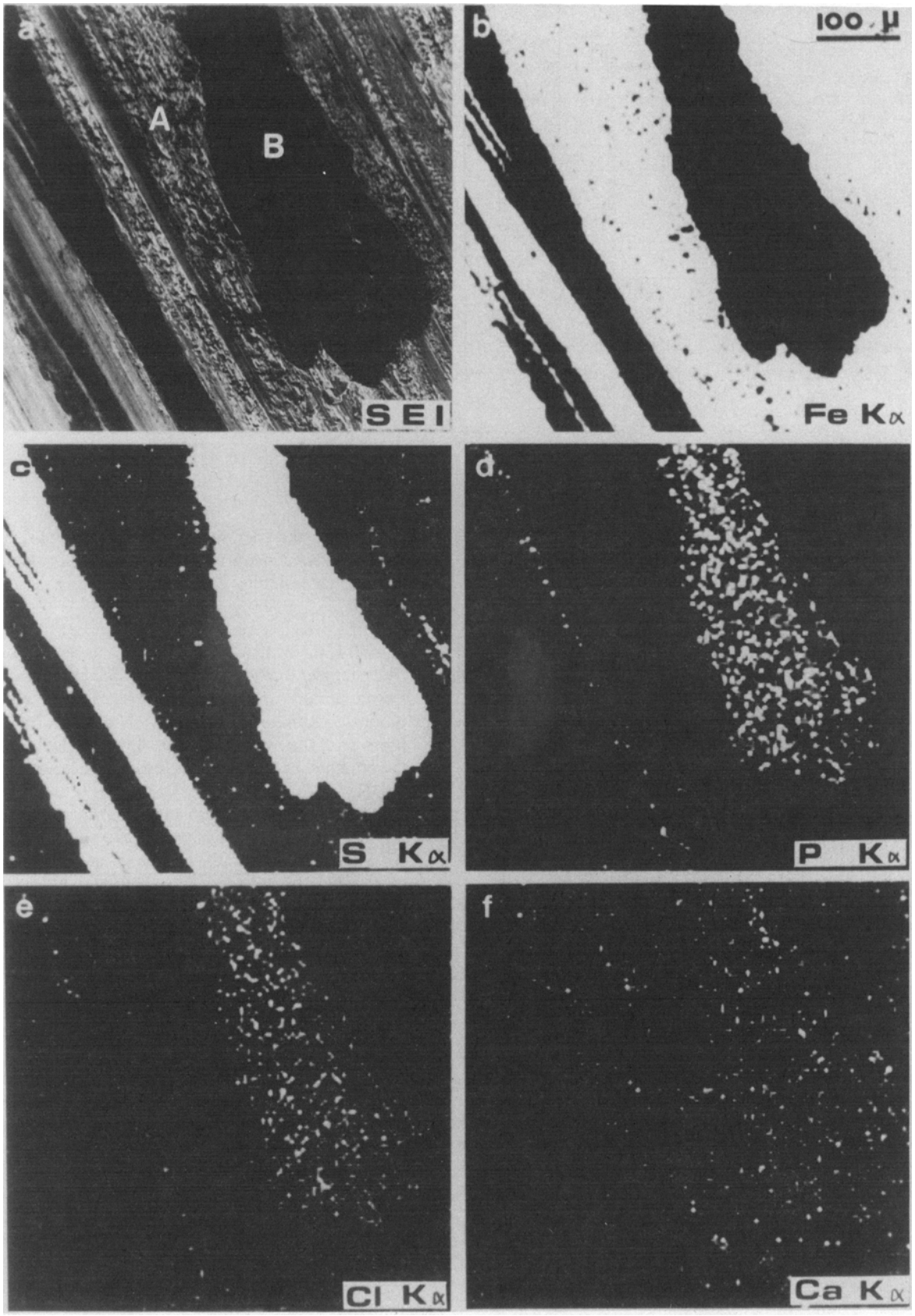

Fig. 15 Scanning electron micrographs. Secondary electron image (a) and X-ray maps of iron (b), sulfur (c), phosphorus (d), chlorine (e), and calcium (f)

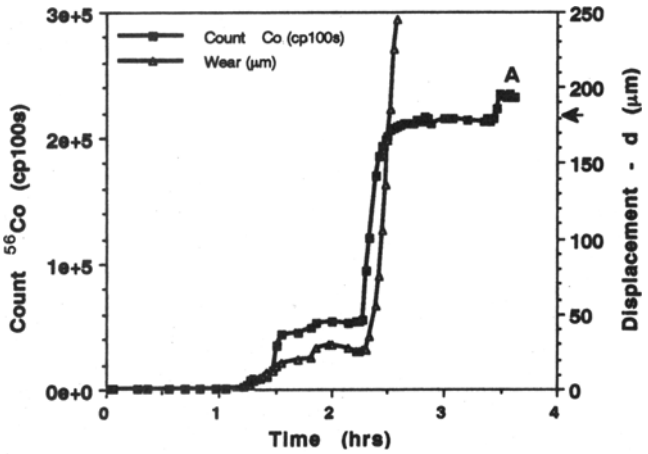

Fig. 16 Cumulative radioactivity measured in the filter and wear vs. real time

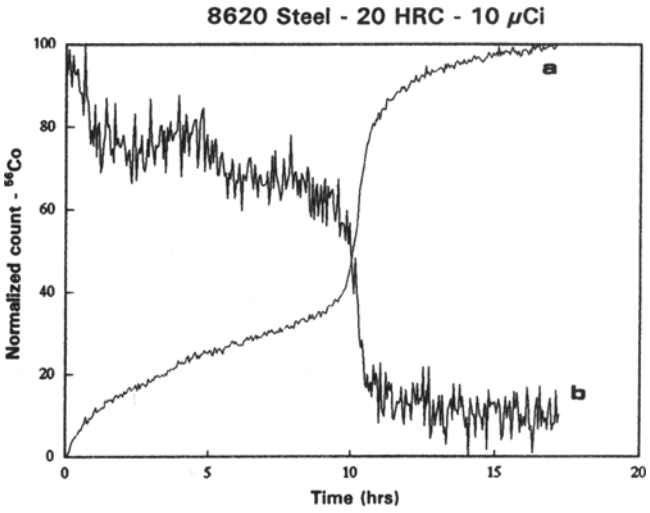

Fig. 18 Cumulative radioactivity measured in the filter (curve a) and residual radioactivity measured in the sample (curve b)

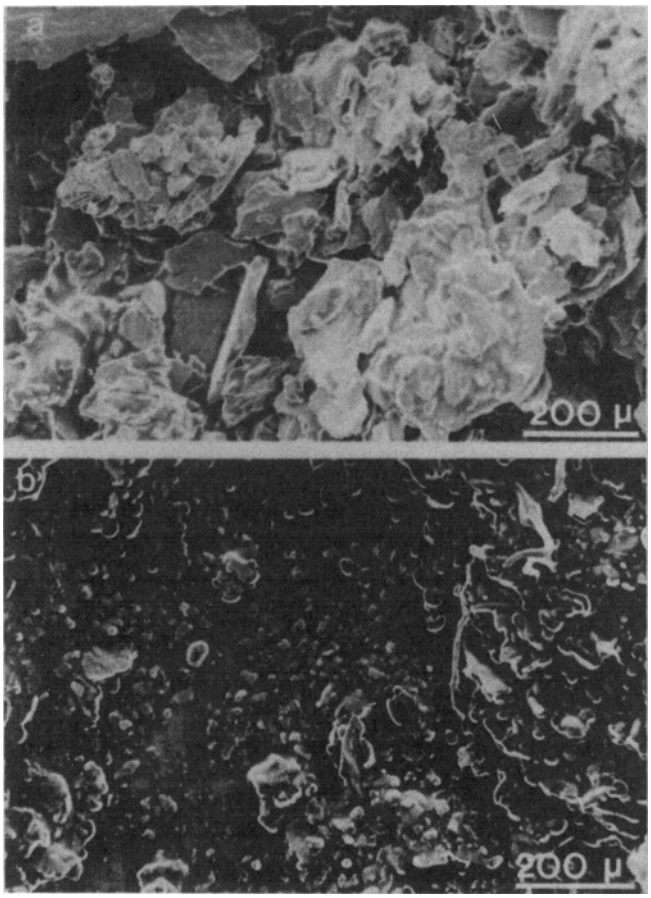

Fig. 17 Scanning electron micrographs of (a) the wear debris particles collected in the filter and (b) wear debris particles filtered from the oil

must be used. Changing any of these parameters requires a new calibration curve to be produced, but this can easily be achieved with the present wear testing system.

4. Conclusions

To reproduce the friction wear conditions (lubricated surfaces) that prevailed in most service cases, we bore in mind two principles when designing the wear testing system:

- The first principle requires that a lubricant film is always present at the contact interface; thus the need of a pressurized chamber (up to 400 psi). In the actual chamber and lubricant circuit, when a load is applied to the system, the lubricated film does not completely disappear, even if the pressure of the fluid equals that of the applied load. This is the principle of hydrostatic or externally pressurized bearing (Ref 11).
- The second principle has to do with ensuring that the moving surfaces are slightly convergent rather than parallel (flat-ended pin with 45° bevel). Thus, the fluid is drawn into a "channel" of reducing cross-sectional area. When this happens to a viscous fluid, a hydrodynamic pressure will develop. This is the principle of the hydrodynamic or self-acting lubricated bearing (Ref 11).

Combined with the great stability of the system with respect to vibration, these two principles allow our testing system to achieve an extremely high level of accuracy.

Acknowledgments

The authors gratefully acknowledge Pratt & Whitney Canada for kindly providing their facilities for plasma spray coating. The authors would also like to thank Jacques Tremblay of LubriLab for kindly providing the tested additive. Finally, we thank Eric Baril for his contribution in carrying out the electron probe microanalysis and Dr. Bruce Kellett for his kind advice about manufacturing the various ceramic samples.

References

1. Design of Friction and Wear Experiments, in Vol 18, *ASM Handbook*, ASM International, 1990, p 480-488

2. S.C. Lim, M.F. Ashby, and J.H. Brunton, *Acta Metall.*, Vol 35 (No. 6), 1987, p 1343-1348
3. H. Czichos, S. Becker, and J. Lexow, *Wear*, Vol 114 (No. 1), 1987, p 109-130
4. ASTM Standard G-99 (1990).
5. Bearing Steels, in Vol 1, *ASM Handbook*, ASM International, 1990, p 380-388
6. "Powder, Plasma Spray, Molybdenum," PWA 1313, Pratt & Whitney Aircraft Group, 1980
7. Lubricant Additives and Their Functions, in Vol 18, *ASM Handbook*, ASM International, 1992, p 98-112
8. T.W. Conlon and B.H. Armitage, The Application of Energetic Ion Beams in the Study of Wear and Porosity, *Wear*, Vol 34, 1975, p 409-418
9. A. Gallmann, B. Natter, and M.A. Molinari, Study of Wear and Galling in Aircraft Fuel Pump Drive Shafts and Gears Using the Surface Layer Activation Technique, *Nuclear Instruments and Methods in Physics Research*, Vol B34, 1988, p 479-482
10. Internal report, Nuclear Physics Laboratory, Université de Montréal, 1993
11. J. Halling, *Introduction to Tribology*, Springer-Verlag, 1976